Status and Performance of the ATLAS Experiment

P. Iengo

LAPP-EXP-2010-03

Status and Performace of the ATLAS Experiment

Paolo Iengo, on behalf of the ATLAS Collaboration[a,*]

[a] *LAPP, Laboratoire d'Annecy-le-Vieux de Physique des Particules, CNRS-IN2P3, 9 Chemin de Bellevue - 74941 Annecy-le-Vieux - FRANCE*

Abstract

ATLAS is a general purpose experiment designed to exploit the full discovery potential of LHC. It consists of an inner detector immersed in a soleinodal magnetic field, hadronic and electromagnetic calorimeters and a muon spectrometer embedded in three air-core toroids. ATLAS registered the first LHC proton-proton collisions at an energy of 900 GeV and 2.36 TeV in the center of mass in December 2009. Since 30 March 2010 the experiment is stably taking data at $\sqrt{s}$ = 7 TeV. The very good state of the ATLAS detector, performance study and first results with collision data are reported.

Keywords: ATLAS, LHC

1. Introduction

The ATLAS experiment [1] is a general purpose detector designed to exploit the full discovery potential of high energy proton-proton and heavy ion collisions from the Large Hadron Collider (LHC). With about 2,900 physicists from 173 Institutions of 37 different Countries, ATLAS is the largest high energy physics Collaboration.

After a commissioning phase with cosmic rays, ATLAS registered the first LHC proton-proton collisions at 900 GeV (the LHC injection energy) and 2.36 TeV in the center of mass in December 2009. Since 30 March 2010 the experiment is stably taking data at the energy of 7 TeV in the center of mass.

This paper reports the state of the ATLAS detector after 31 nb^{-1} recorded with stable beams at $\sqrt{s}$ = 7 TeV with emphasis on detector performance and first results with collision data.

2. The ATLAS detector

The ATLAS detector (44m long, 25m high with a weight of about 7,000 tonnes) is the largest detector ever built at an accelerator. Its layout, shown in Figure 1, comprises an inner detector system immersed in a 2 Tesla solenoidal magnetic field, electromagnetic and hadronic calorimetry, and an outermost muon spectrometer embedded in three superconducting air-core toroids with a typical field of 0.5T in the barrel and 1T in the end-caps.

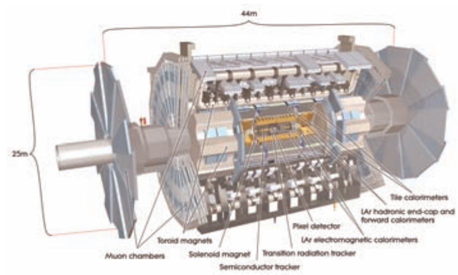

Figure 1: Cut-away view of the ATLAS detector

The ATLAS detector covers almost the whole solid angle up to pseudorapidities $|\eta|$= 4.9 for the calorimetric and $|\eta|$= 2.5 for tracking measurements. The trigger chain of the experiment allows to reduce the expected nominal interaction rate of about 1 GHz (with a bunch crossing rate of 40 MHz) to an output rate of few hundreds hertz. It is structured in three decision levels: the LVL1 (hardware implemented with trigger boards mounted on-detector) is based on local information from the Muon Spectrometer and calorimeters with coarse granularity and defines the region of interest of the detector; the following trigger levels (LVL2 and Event Filter) are software based. They use the full detector granularity, perform the track matching with the inner detector and the full event building.

---
*Speaker

Email address: paolo.iengo@cern.ch (Paolo Iengo, on behalf of the ATLAS Collaboration)

The main characteristics of the ATLAS sub-detectors are summarized in the following sub-sections.

2.1. Inner Detector

The Inner Detector designed to precisely measure the tracks of charged particles and reconstruct the decay vertices is built of three pixel layers, four double-sided silicon micro strip detectors (SCT) in the barrel and nine in each end-cap, and, in the external part, a transition radiation tracker (TRT) based on straw tubes with electron-pion separation capability. The Inner Detector covers a region $|\eta|<2.5$; the expected momentum resolution is $\sigma_{p_T}/p_T = 3.8 \times 10^{-4} p_T \oplus 0.015$ for particles at $|\eta|=0$, while the impact parameter resolution is expected to be $\sigma_{d_0} \sim 10 \oplus 140/p_T(GeV)\mu m$.

2.2. Calorimeters

The electromagnetic (EM) calorimeter provides triggering, identification and energy measurement of electrons and photons. It is a sampling calorimeter using the lead/liquin Argon (LAr) technology. It has an accordeon geometry, for a full ϕ hermeticity, covering $|\eta|<3.2$. The energy resolution is $\sigma_E/E = 10\%/\sqrt{E} \oplus 0.7\%$.

The hadronic calorimeter extends up to $|\eta|<4.9$. It is made of iron with scintillator tiles in the barrel region, with a resolution of $\sigma_E/E = 50\%/\sqrt{E} \oplus 0.03$. In the two end-caps the hadronic calorimeter is based on liquid Argon with copper/tungsten absorbers, with a coverage $1.5 <|\eta|<3.2$. In the same cryostats the forward calorimeter ($3.2 <|\eta|<4.9$), designed to detect hadron jets at angles from 1 to 5 degrees relative to the proton beams, also based on LAr, are hosted.

2.3. Muon System

Precision measurement of muon tracks in the bending coordinate is carried out by Monitored Drift Tube (MDT) chambers with an η coverage up to 2.7, complemented by Cathode Strip Chambers (CSC) in the highest rapidity region. The muon trigger is based on Resistive Plate Chambers (RPC) in the barrel region ($|\eta|<1.05$) and Thin Gap Chambers (TGC) in the end-caps ($1.05 <|\eta|<2.07$). Trigger chambers also provide position measurement in non-bending plane.

The spatial resolution is better than 100μm in the bending plane and of the order of 10mm in the ϕ direction. The overall momentum resolution is better than 10% for particle transverse momentum up to 1 TeV.

3. Detector performance

Since 30 March 2010 ATLAS is stably taking data at 7 TeV. In the first three months of activity the experiment has collected 31.04nb^{-1} in stable beam conditions with a data taking efficiency of about 92% and an average operating fraction of 98%.

All the components of ATLAS have shown very good performance and a behavior close to the expected one. The performance of the tracker can be determined by reconstructing hadron resonances like K_s^0, Λ etc. These studies allow the determination of the momentum scale, the detector resolution and the estimation of the material budget. As an example fig. 2 shows the K_s^0 mass peak obtained by combining oppositely charged tracks with a common vertex and with the hypothesis of being pions. The measured value of the mass (497.5 ± 0.1)MeV is in perfect agreement with the PDG value and the data is well reproduced by the Monte Carlo.

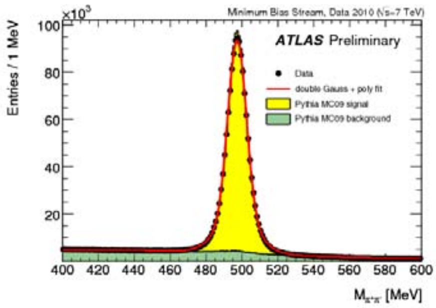

Figure 2: Invariant mass of two charged pions in the K_s^0 mass peak region.

TRT electron-pion separation capability is shown in fig. 3 . The plot represents the probability of having an hit with high threshold in the TRT as a function of the γ factor of the particle. The separation of electrons and pions is evident and the detector response is in good agreement with the expectations.

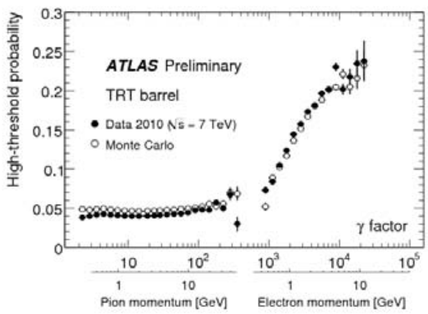

Figure 3: Probability of an high threshold hit in the Transition Radiation Tracker.

In a similar way, the the electromagnetic energy scale and the performance of the electromagnetic calorimeter can be studied by reconstructing the γ-γ or the electron-electron invariant mass. Figure 4 top shows the π^0 mass peak obtained applying a cut of 0.4 GeV on the cluster transverse energy and of 0.9 GeV on the transverse momentum of the photon pair. To identify the cluster as a photon it is required to not match a track in the inner detector. The agreement between data and Monte Carlo better than 2% is a great achievement considering the low mass of the π_0 and that the result has been derived with the very first data of the experiment.

Figure 4 bottom shows the data/MC comparison for one of the electron identification variable, i.e. the shower shape in the second layer of the EM calorimeter, including the expected contributions from prompt electrons, electrons from conversions and from hadrons. The variable R_η is defined as the ratio between the energy contained in a region $\Delta\eta \times \Delta\phi = 3 \times 7$ cells around the hottest cell and the energy in a region 7×7.

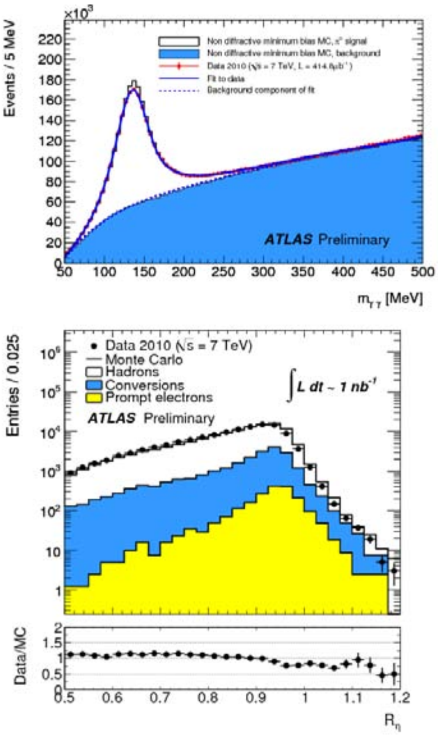

Figure 4: Top: Invariant mass of photon pairs. The π_0 mass peak is evident. Bottom: Electron shower shape in the second layer of the electromagnetic calorimeter.

Good agreements of data and Monte Carlo expectations have been also found for missing energy and jets variables. Figure 5 shows transverse energy distribution (top) for an integrated luminosity of 0.3 nb^{-1} and the jet p_T distribution (bottom) for 1 nb^{-1} with the break-down of the contributions from jets from light, c and b quarks.

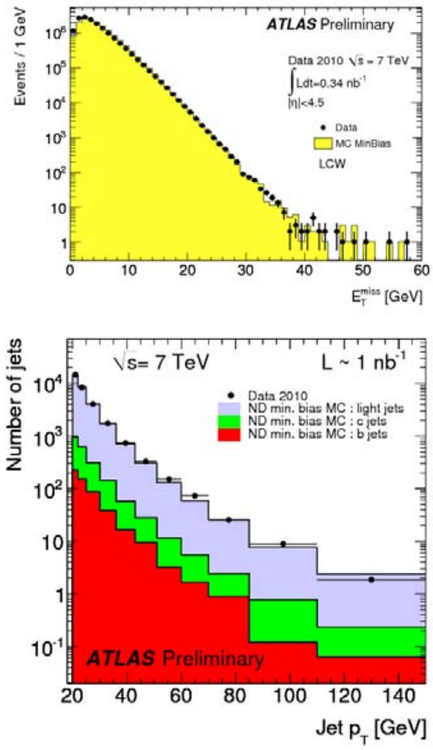

Figure 5: Top: distribution of missing transverse energy. Bottom: Jet transverse momentum distribution. The expected contribution from light jets, c and b jets are also shown.

ATLAS can reconstruct muons separately in the Muon Spectrometer and in the Inner Detector. The two tracks can be matched to obtain a *combined* muon. The di-muon invariant mass distribution, corresponding to the J/ψ peak for 9.5nb^{-1}, is shown in fig. 7 top. Here muon pairs with opposite charge, a common vertex and energy above 3 GeV are selected with the additional request that at least one of the two muon is a combined muon. Figure 6 bottom shows the muon trigger efficiency for the J/ψ candidates as a function of the transverse momentum p_T. The efficiency curve reaches a plateau (>95%) for p_T of the J/ψ candidates larger than 10 GeV.

4. Observation of *Z* and *W*

The excellent status of the ATLAS detector is confirmed by the early observation of W and Z bosons decays in leptonic channels. The first W candidate has been found few days after the first 7 TeV proton-proton collision in

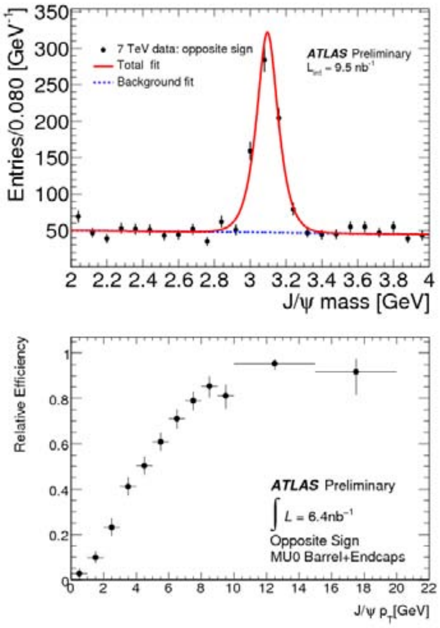

Figure 6: Top: Invariant mass of muon pairs; the peak correspond to the $J\Psi$ resonance. Bottom: Muon trigger efficiency for $J\Psi$ cndidates.

ATLAS and few weeks later the first W candidate was observed. As an example fig. 7 shows the event display for a $W \rightarrow e\nu$ (top) and a $Z \rightarrow \mu\mu$ (bottom) candidate. In the W event the measured electron transverse momentum is 23 GeV, the reconstructed missing transverse energy is 31 GeV and the reconstructed transverse mass of the W is 55 GeV. In the Z event the negative muon is detected in the barrel part of the Spectrometer with p_T = 27 GeV and the positive one in the end-cap p_T = 45 GeV; the invariant mass of the Z candidate is reconstructed to be 87 GeV.

5. Conclusions

After an intense commissioning work the ATLAS experiment has recorded the first LHC proton-proton collisions in fall 2009 and is now stably collecting data at 7 TeV center-of-mass energy. The experiment is working extremely well, with a data taking efficiency larger than 90%, along with the data distribution and the analysis infrastructure.

Detector performance studies have shown impressive agreement with Monte Carlo expectation for all the ATLAS sub-systems and first physics measurements have been performed [2] . W and Z have been observed soon after the first collision at $\sqrt{s}$ = 7 TeV and a large statistic is now being accumulated opening the electroweak sector of LHC physics.

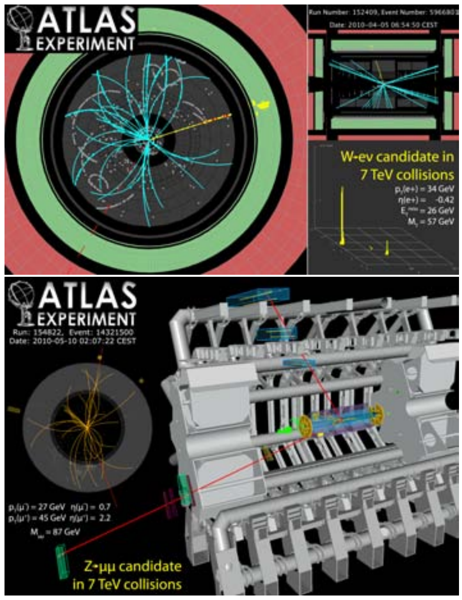

Figure 7: Top: Invariant mass of muon pairs; the peak correspond to the $J\Psi$ resonance. Bottom: Muon trigger efficiency for $J\Psi$ cndidates.

The LHC physics era has just begun and ATLAS has started to exploit its full physics potential.

Acknowledgements

I would like to thank the QCD-10 conference organizers for the interesting conference and the LPTA-Montpellier for hospitality.

References

[1] The ATLAS Collaboration, G. Aad et al., The ATLAS Experiment at the CERN Large Hadron Collider, JINST 3 (2008) S08003.

[2] The ATLAS Collaboration, G. Aad et al., Phys.Lett.B688:21-42,2010.